Zhao *et al. EURASIP Journal on Wireless Communications and Networking* (2018) 2018:275
https://doi.org/10.1186/s13638-018-1297-9

EURASIP Journal on Wireless Communications and Networking

RESEARCH Open Access

Performance analysis for high-speed railway distributed antenna systems with imperfect channel state information

Jing Zhao[1*], Jingxian Wu[2] and Pingzhi Fan[1]

Abstract

This paper studies the performance of antenna selection for high-speed railway (HSR) distributed antenna systems with imperfect channel state information (CSI). In HSR systems, distributed antennas mounted on top of the train carriage are connected to a mobile relay, which serves as an intermediate node between the base station (BS) and the users inside the train. An important feature of high mobility networks is the fast time-variation of the fading channel caused by the large Doppler spread. It is difficult to accurately estimate, track, and predict the fast time-varying fading coefficients; thus, channel estimation error is usually inevitable and it may seriously degrade system performance. In order to offer a good tradeoff between system performance, cost, and overhead, antenna selection is performed by considering the impacts of both channel estimation errors and noise, such that the antenna with the best link to the BS will be selected to serve users inside the train. The channel estimation error is quantified through the estimation mean squared error (MSE), which is expressed as a closed-form function of the maximum Doppler spread and signal-to-noise ratio (SNR). Several performance metrics, such as outage probability, symbol error rate, spectral efficiency lower bound, and switching rate, are developed as a function of the channel estimation MSE and the geometric layout of the antennas. The analytical and simulation results quantify the significant impacts of imperfect CSI on antenna selection for HSR systems in practical applications.

Keywords: Distributed antenna selection, Mobile relay, High-speed railway, Channel estimation errors

1 Introduction

With the increasing popularity of high-speed railway (HSR) systems around the world, it is important to provide broadband reliable wireless communication to passengers onboard high-speed trains. A significant problem, however, is that radio signals traveling from the base station (BS) into the train are severely attenuated by the vehicular penetration loss (VPL). Depending on the age and type of the coach, the degree of attenuation can vary from −5 to −35 dB [1, 2]. The performance of HSR communication systems can be improved by employing mobile relay (MR) mounted on top of the train [1–5]. MR serving as an intermediate relay can assist the on-board passengers to communicate with the BS at high data rate despite travelling at high velocity. In the uplink, it can congregate information from all users in the train and deliver them to the BS. In the downlink, the MR retransmits the signal from BS to the user equipment (UE) through wireless links. Furthermore, MR can effectively circumvent the high penetration loss of the carriages and significantly reduce the overhead by congregating signals from a large number of users. In addition, the UE is relatively close to the MR; thus, the transmission power of the UE can be reduced.

Deploying multiple antennas can provide spatial diversity to enhance the transmission reliability and capacity for HSR networks. Since a train is usually longer than 200 meters, it can provide sufficient space for installing multiple antennas in the form of a linear array. On the other hand, to reduce the cost and operation overheads, we can explore the space diversity by using antenna selection [6], that is, allocate all resources to the antenna with

*Correspondence: kettyzj@163.com
[1]Institute of Mobile Communications, Southwest Jiaotong University, 610031 Chengdu, Sichuan, People's Republic of China
Full list of author information is available at the end of the article

the best link quality to the BS to improve system performance, which requires the knowledge of channel state information (CSI). However, high mobility networks usually experience fast time-varying fading caused by large Doppler shifts. The fast fading variation imposes tremendous challenges to the accurate estimation and tracking of the time-varying CSI [7]. Therefore, channel estimation errors are inevitable in HSR systems and they will have significant impacts on system performance [8–10]. In high-mobility networks, channel estimation error is caused by two factors: distortions due to noise and outdated CSI due to fast fading variation.

The presence of imperfect CSI is especially detrimental to antenna selection systems, which rely on the CSI to pick the antenna with the best signal-to-noise ratio (SNR). Hence, in order to further improve the performance, antenna selection is developed by considering the impacts of channel estimation errors and the geometric layout of the antenna array. Different antenna selection and relay selection schemes with imperfect CSI have been studied in [11–13]. The effect of outdated CSI on the outage and error rate performance of amplify-and-forward (AF) relay selection was discussed in [11]. Seyfi et al. [12] investigated the performance of selection cooperation in the presence of imperfect channel estimation. In [13], the outage probability and the asymptotic behavior of decode-and-forward (DF) relay selection with outdated channel estimates was studied. However, the effect of imperfect CSI on the switching rate, which is an important indicator for selection combining scheme, has not been studied in the literature. Furthermore, these existing works only consider traditional multiple-input multiple-output system with co-located antennas, or multiple fixed relays with single antenna, and they do not consider the effects of pathloss or geometric layout of the antenna array, which have significant impacts on the performance of HSR systems. In addition, the impacts of user mobility or Doppler spread on the system performance is not studied either. Therefore, the existing results cannot be readily applied to HSR systems with distributed antennas.

This paper addresses the performance of an antenna selection scheme in a distributed antenna setup. The objective is mainly to evaluate the antenna selection algorithm against fast channel variations due to high mobility of the trains. Antenna selection relies on future CSI, which is estimated and predicted by using pilot symbols at the current slot following the minimum mean squared error (MMSE) or the maximum likelihood (ML) criterion. The impacts of both noise distortion and outdated channel information are considered during channel estimations. We quantify the performance of the antenna selection system by developing analytical expressions of the outage probability (OP), the symbol error rate (SER), an average spectral efficiency lower bound, and the switching rate. They are expressed as explicit functions of a number of system parameters, such as the channel estimation MSE related to the train speed, the average SNR, and the distance between the mobile antennas and the BS. The impacts of high mobility and channel estimation errors on system performance are investigated through both analytical and simulation studies.

The main contributions of this paper can be summarized as follows:

- A new antenna selection scheme for HSR systems is introduced. The antenna selection is performed by considering both the impacts of imperfect CSI due to high mobility of the train and the geometric layout of the distributed linear antenna array mounted on top of the train. Unlike existing antenna selection schemes for co-located antennas, the proposed scheme considers the effects of different pathloss experienced by distributed antennas, and this leads to significant performance gains over conventional systems.
- The impacts of train mobility on system performance are explicitly quantified by analytically identifying the relationship between train speed and channel estimation error. The results are used to develop an analytical OP, SER, a spectral efficiency lower bound, and switching rate for systems operating with imperfect CSI.

2 Methods

The rest of this paper is organized as follows. Section 3 presents the system model of a high-speed railway communication system with distributed antennas and illustrates how high mobility and long distance impact on the channel model. In Section 4, a novel antenna selection scheme with imperfect CSI is proposed by using a pilot-assisted MMSE channel prediction, following by the study of the statistical properties of channel estimation error, which is based on the features of HSR networks. By employing the theory of probability and integrals and the probability density function (pdf) of random variables, performance analysis is performed in Section 5 by developing the OP, SER, spectral efficiency lower bound, and switching rate of the HSR communication system. Section 6 provides the Monte-Carlo simulation in MATLAB to verify the obtained analytical results. Section 7 concludes the whole paper.

3 System model

Consider a two-hop network structure for the railway communication system as shown in Fig. 1. Since high-speed trains move along a near liner rail, cells can be laid out along the route in one-dimension instead of the two-dimensional hexagonal zones in conventional

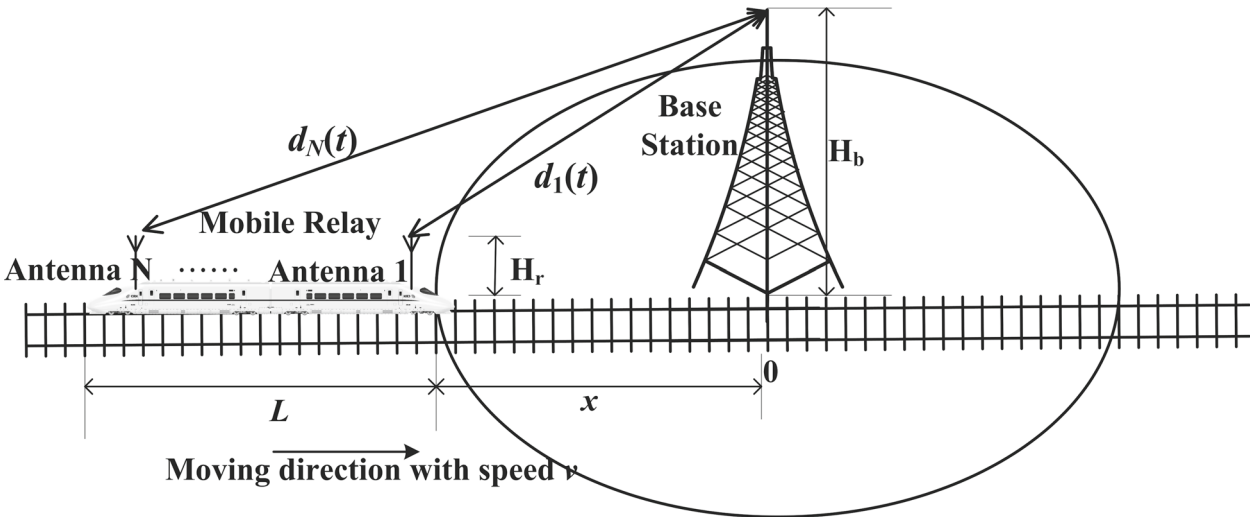

Fig. 1 The system model for HSR systems

cellular systems [14, 15]. As a result, each cell in the HSR system has only two neighboring cells instead of six neighboring cells as in a conventional hexagonal cellular structure. Thus, the effects of adjacent cell interference (ACI) or co-channel interference (CCI) from neighboring cells are much smaller compared to conventional cellular structure. In addition, the small number of neighboring cells allows a more generous frequency reuse scheme because the spectrum resources only needed to be share with fewer cells. In this paper, it is assumed that adjacent cells employ different spectrum. Thus, the effects of ACI or CCI is negligible. The UE onboard the train communicates with the BS by using MR with a linear array of distributed antennas mounted on top of the train as relays. Since MR only needs to provide coverage to users inside the train and the MR and UEs are relatively static and close to each other, it can be seen that the BS-MR link communication capability is the bottleneck of the HSR system. Assume that the capacity of the MR-UE link is much larger than that of the BS-MR link. Thus, we will focus on the study of the BS-MR antenna links, which limit the overall system performance.

In order to offer a good tradeoff between system performance and operation cost, this framework adopts antenna selection, wherein the mobile relay chooses one of the distributed antennas for uplink communication, preferably the one that yields the highest effective SNR among all of them. Due to the high mobility of the train, the system can only have an inaccurate estimate of the SNR based on imperfect CSI. The MR antenna with the best estimated SNR assists the users inside the train to transmit to BS, and all the transmitted data and available power will be aggregated at the best MR antenna. Assume the system employs time division duplex (TDD) such that the uplink-downlink channel reciprocity can be utilized. The MR will estimate the downlink CSI for all antennas with the assist of pilot symbols transmitted by the BS. The estimated downlink CSI will then be used to predict the uplink CSI in the next time slot. In a high-speed train system, large Doppler spread caused by high mobility of the train introduces fast time-varying fading. Consequently, the CSI of two consecutive time slots are correlated but different.

The downlink signal observed by the n-th MR antenna during the k-th symbol period is

$$y_n(k) = \sqrt{E_n} h_n(k) x_k + z_n(k) \tag{1}$$

where x_k is a modulated pilot or data symbol with unit energy, $z_n(k)$ is additive white Gaussian noise (AWGN) with variance σ_z^2, $E_n = E_0 d_n^{-\alpha}$ is the average received symbol energy at the n-th MR antenna, with E_0 being the transmission energy and d_n the distance between the BS and the n-th MR antenna, and $h_n(k)$ is the time-varying small-scale fading. In Rayleigh fading channel, $h_n(k)$ is a zero-mean complex Gaussian random process with the auto-correlation function [16]

$$\rho = \mathbb{E}\left[h_n(k) h_n(l)^*\right] = J_0\left(2\pi f_{\mathrm{D}} \cos\theta_n |k-l| T_s\right) \tag{2}$$

where f_{D} is the maximum Doppler spread, θ_n is the angle between the train's moving direction, and the BS-MR line, T_s is the symbol period, and $J_0(x)$ is the zero-order Bessel function of the first kind.

Assume that the BS is d_v meters away from the rail tracks, and the antenna of the BS is H_b meters above the ground. Denote the length of the train as L and there are

N MR antennas evenly distributed on top of the train. The MR antennas are H_r meters above the ground. Without loss of generality, it is assumed that the horizontal coordinate of the BS is 0. Let x be the horizontal coordinate of the head of the train, then the coordinate of the n-th MR antenna is $x_n = x - \frac{(n-1)}{N-1}L$. The distance between the BS and the n-th MR antenna is thus $d_n(x) = \sqrt{|x_n|^2 + d_0^2}$, where $d_0 = \sqrt{(H_b - H_r)^2 + d_v^2}$, for $n = 1, \ldots, N$.

4 Antenna selection based on imperfect CSI

This section presents the proposed antenna selection scheme, where the best antenna is selected by predicting the uplink CSI with the estimated CSI in the downlink. In HSR systems, since the channel between the train and the BS changes at a higher rate, it is needed to predict the SNR in the next time slot by using the pilot symbols received at the current slot. Using channel prediction instead of simple channel estimation can avoid the use of stale CSI for antenna selection, thus achieving better performance. Firstly, the pilot-assisted channel estimation algorithms are discussed for channel prediction, studying the statistical properties of the imperfect CSI. The results are then used to develop the antenna selection algorithm.

4.1 Statistical properties of imperfect CSI

Due to the temporal channel correlation, the channel coefficients of the next slot can be predicted by using the pilot symbols received at the current slot. The channel prediction involves two steps. At the first stage, the MR estimates the downlink CSI of the current time slot with the help of pilot symbols. Then, the MR predicts the uplink CSI of the next time slot at the second stage. During the analysis, it is assumed that the channel remains constant in one time slot, the duration of which is usually much smaller than the channel coherence time, even in high mobility systems.

The channel estimation can be performed by following either the MMSE or the ML criteria. We will study channel estimation under both criteria and compare their performance.

4.1.1 MMSE channel estimation

Assume $x_k = p$ is a pilot symbol in the downlink. Without loss of generality, it is assumed that the pilot symbols are from a constant amplitude alphabet set, that is $|p|^2 = 1$.

The MMSE channel estimation of $h_n(k)$ by the n-th MR antenna is

$$\begin{aligned}\hat{h}_n(k) &= \mathbb{E}\left[h_n(k)y_n(k)^*\right] \cdot \mathbb{E}\left[y_n(k)y_n(k)^*\right]^{-1} \cdot y_n(k) \\ &= \sqrt{E_n}p^*\left(E_n + \sigma_z^2\right)^{-1} y_n(k)\end{aligned} \tag{3}$$

Once the downlink CSI of the current slot is estimated, the result is then used to predict the uplink CSI of the next slot by following the MMSE criterion. The predicted uplink CSI at time instant l is

$$\tilde{h}_n(l) = w_n(k,l)\hat{h}_n(k) \tag{4}$$

where $w_n(k,l)$ is the MMSE coefficient. Based on the orthogonal principle, $\mathbb{E}\left\{\left[w_n(k,l)\hat{h}_n(k) - h_n(l)\right]\hat{h}_n^*(k)\right\} = 0$, it can be presented as

$$w_n(k,l) = \mathbb{E}\left[h_n(l)\hat{h}_n^*(k)\right]\mathbb{E}\left[\hat{h}_n(k)\hat{h}_n^*(k)\right]^{-1} \tag{5}$$

If assume that the duration of one slot is $T_0 = (l-k)T_s$, then the MMSE prediction of $h_n(l)$ can be obtained by combining (3), (4), and (5), and the result is

$$\tilde{h}_n^{\mathrm{MMSE}}(l) = \sqrt{E_n}J_0(2\pi f_n T_0)p^*\left(E_n + \sigma_z^2\right)^{-1} y_n(k) \tag{6}$$

where $f_n = f_\mathrm{D}\cos\theta_n$. Define $e_n = \tilde{h}_n(l) - h_n(l)$. Then, the mean squared error (MSE), $\sigma_n^2 = \mathbb{E}\left(|e_n|^2\right)$, is

$$\sigma_{n,\mathrm{MMSE}}^2 = 1 - J_0^2\left(2\pi f_n T_0\right)\left(1 + \frac{1}{\gamma_n}\right)^{-1} \tag{7}$$

where $\gamma_n = \frac{E_n}{\sigma_z^2} = \frac{E_0 d_n^{-\alpha}}{\sigma_z^2}$ is the average downlink SNR at the n-th MR antenna.

4.1.2 ML channel estimation

Under the assumption of Rayleigh fading, for a fixed pilot symbol, the observation $y_n(k)$ and the fading channel $h_n(k)$ are jointly Gaussian distributed. Since $h_n(k)$ and $h_n(l)$ are also jointly Gaussian distributed, we have that $y_n(k)$, $h_n(k)$, and $h_n(l)$ are jointly Gaussian distributed. The mean and variance of $y_n(k)$ are

$$\mathbb{E}\left[y_n(k)\right] = \mathbb{E}\left[h_n(k)\right]p + 0 = 0 \tag{8}$$

$$\mathbb{E}\left[|y_n(k)|^2\right] = E_n\mathbb{E}\left[|h_n(k)|^2\right]|p|^2 + \sigma_z^2 = E_n + \sigma_z^2 = \sigma_y^2 \tag{9}$$

In addition, the cross-correlation between $y_n(k)$ and $h_n(l)$ is

$$\mathbb{E}\left[y_n(k)h_n^*(l)\right] = \sqrt{E_n}J_0(2\pi f_n T_0)p \tag{10}$$

Therefore, the likelihood function $p(y_n(k)|h_n(l))$ is a Gaussian probability density function (pdf), with the conditional mean $\mu_{y_n(k)|h_n(l)}$ and conditional variance $\sigma^2_{y_n(k)|h_n(l)}$, given by

$$\mu_{y_n(k)|h_n(l)} = \sqrt{E_n}pJ_0(2\pi f_n T_0)h_n(l) \tag{11}$$

$$\sigma^2_{y_n(k)|h_n(l)} = E_n + \sigma_z^2 - E_n J_0^2(2\pi f_n T_0) \tag{12}$$

Then, the ML prediction of $h_n(l)$ can be obtained by

$$\tilde{h}_n^{\mathrm{ML}}(l) = \arg\max p(y_n(k)|h_n(l)) = \frac{y_n(k)}{\sqrt{E_n}pJ_0(2\pi f_n T_0)} \tag{13}$$

The variance of the channel estimation error can then be calculated as

$$\sigma^2_{n,\mathrm{ML}} = \frac{1}{J_0^2\left(2\pi f_n T_0\right)}\left(1+\frac{1}{\gamma_n}-J_0^2(2\pi f_n T_0)\right) \tag{14}$$

The variances of the channel estimation errors of MMSE and ML estimation are compared in Figs. 2 and 3, for systems with $f_\mathrm{D}T_s = 0.01$ and 0.1, respectively. In both cases, the MMSE estimation outperforms ML estimation, and the performance difference is bigger at higher $f_\mathrm{D}T_s$. Thus, the MMSE algorithm is better than the ML algorithm, especially under high mobility environment. Thus, in the following analysis, we will focus on the results obtained from the MMSE channel estimation.

In (7), the channel estimation MSE is expressed as an explicit function of the maximum Doppler spread, the duration of a slot, and the location of the train. The function $J_0(2\pi x)$ is decreasing in x for $x \in [0, 0.3827)$. In practical systems, we usually have $f_n T_0 \ll 0.3827$. For a system with symbol rate 100 ksym/s and operating at 1.9 GHz, the range of the Doppler spread is between 100 Hz ($f_n T_0 = 10^{-3}$) to 1 KHz ($f_n T_0 = 10^{-2}$), which correspond to a mobile speed in the range between 56.8 and 568.4 km/hr [8]. Thus, $J_0\left(2\pi f_n T_0\right)$ decreases in $f_n T_0$ for practical values of $f_n T_0$. At a given location, σ_n^2 is an increasing function in $f_n T_0$ for $f_n T_0 < 0.3827$, which means that a higher train mobility will result in a higher MSE. At a given train speed or f_D, when the MR antenna is closer to the BS, γ_n is larger and f_n is larger, there is an optimum position which results in a smaller σ_n^2.

Conditioned on the pilot symbol p, the observed pilot symbol $y_n(k)$ is Gaussian distributed. Since $\tilde{h}_n(l)$ is a linear transformations of $y_n(k)$, it is also Gaussian distributed. From (6), the mean of $\tilde{h}_n(l)$ is 0, and its variance is $1-\sigma_n^2$.

4.2 Distributed antenna selection scheme

Based on the statistical properties of the estimated channel coefficients, the system equation for uplink transmission can be written as

$$y_n(l) = \sqrt{E_n}[\,\tilde{h}_n(l) + e_n]\,x_l + z_n. \tag{15}$$

Considering the effects of imperfect CSI, the effective SNR for the n-th MR antenna is given by

$$\hat{\gamma}_n = \frac{E_n\left|\tilde{h}_n(l)\right|^2}{E_n\sigma_n^2+\sigma_z^s} = \frac{\gamma_n\left|\tilde{h}_n(l)\right|^2}{\gamma_n\sigma_n^2+1} \tag{16}$$

During the uplink transmission, the central unit on the train will select the MR antenna with the best effective SNR $\hat{\gamma}_n$ as follows:

$$k = \arg\max_n(\hat{\gamma}_n),\quad n = 1,\ldots,N \tag{17}$$

After distributed antenna selection with imperfect CSI, the effective SNR of uplink transmission can be presented as

$$\hat{\gamma}_{\max} = \max_n \hat{\gamma}_n = \hat{\gamma}_k \tag{18}$$

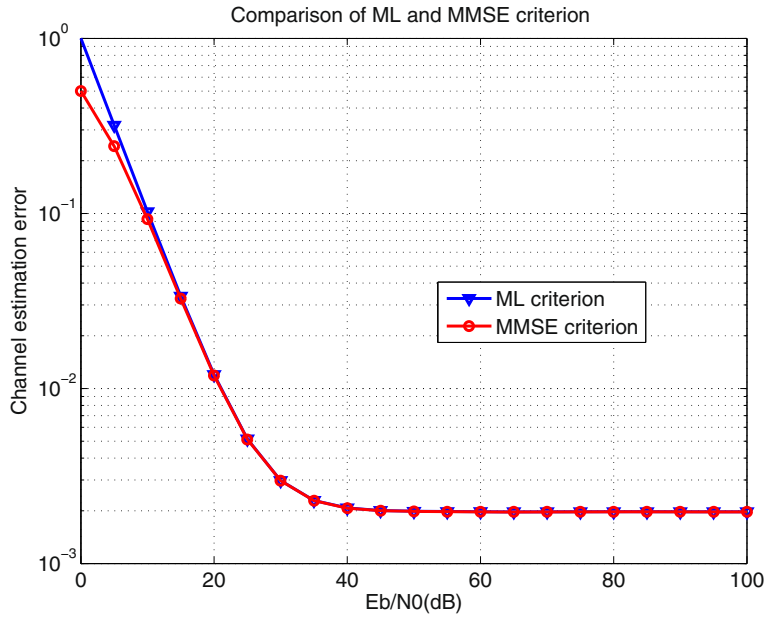

Fig. 2 Comparison of ML and MMSE criterion with $f_\mathrm{D}T_s = 0.01$

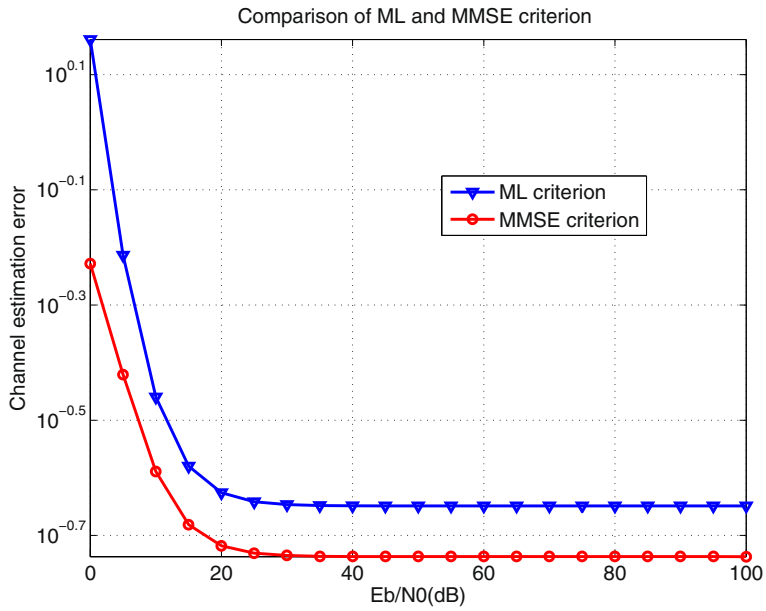

Fig. 3 Comparison of ML and MMSE criterion with $f_D T_s = 0.1$

5 Performance analysis

The performance of the proposed antenna selection scheme is studied in this section. Specifically, the analytical expressions of outage probability, average symbol error probability, spectral efficiency lower bound, and switching rate will be developed, by considering the analytical properties of imperfect CSI.

5.1 Outage probability

The outage probability P_{out} is defined as the probability that the system cannot support a certain target data rate. It is equivalent to the probability that the overall effective SNR is lower than a threshold, γ_T, which is related to the target rate R via $\gamma_T = 2^{2R} - 1$. For the proposed distributed antenna selection system under the high mobility scenario, the outage probability is given by

$$P_{\text{out}} = P\left(\hat{\gamma}_{\max} \leq \gamma_T\right) = F_{\hat{\gamma}_{\max}}(\gamma_T) \tag{19}$$

where $F_{\hat{\gamma}_{\max}}(x)$ is the cumulative distribution function (CDF) of $\hat{\gamma}_{\max}$. Since $\tilde{h}_n(l)$ is zero-mean Gaussian distributed with variance $1 - \sigma_n^2$, the effective SNR $\hat{\gamma}_n$ given in (16) is expontially distributed. From (16), the mean of $\hat{\gamma}_n$ is

$$\beta_n = \mathbb{E}(\hat{\gamma}_n) = \frac{\gamma_n\left(1-\sigma_n^2\right)}{\gamma_n\sigma_n^2 + 1} \tag{20}$$

Combining (7) and (20) yields

$$\beta_n = \left[\left(1+\frac{1}{\gamma_n}\right)^2 \frac{1}{J_0^2(2\pi f_n T_0)} - 1\right]^{-1} \tag{21}$$

It is obvious that β_n increases in γ_n, and decreases in $f_n T_0$ when $f_n T_0 < 0.3827$.

The CDF of $\hat{\gamma}_n$ is thus

$$F_{\hat{\gamma}_n}(\gamma) = 1 - \exp\left(-\frac{\gamma}{\beta_n}\right) \tag{22}$$

Since $\hat{\gamma}_n$ are mutually independent, the CDF of $\hat{\gamma}_{\max}$ is

$$F_{\hat{\gamma}_{\max}}(\gamma) = \prod_{n=1}^{N} F_{\hat{\gamma}_n}(\gamma) = \prod_{n=1}^{N}\left[1 - \exp\left(-\frac{\gamma}{\beta_n}\right)\right] \tag{23}$$

From (7), (20), and (23), the outage probability can be expressed by

$$P_{\text{out}} = \prod_{n=1}^{N}\left[1 - \exp\left(\frac{(1+\gamma_n)^2\gamma_T}{\gamma_n^2 J_0^2(2\pi f_n T_0)} - \gamma_T\right)\right] \tag{24}$$

5.2 Average symbol error rate

The average symbol error rate (SER) of the proposed distributed antenna selection scheme in the presence of imperfect CSI is derived in this subsection. It is shown in [12] that the average SER in many digital modulation scenarios over fading channel is given by

$$\bar{P}_e = \int_0^{\infty} bQ\left(\sqrt{a\gamma}\right) f_\gamma(\gamma)\, d\gamma \tag{25}$$

where $Q(x)$ is the Gaussian-Q function, and the values of a and b depend on the modulation scheme. For instance, for BPSK modulation $a = 2$ and $b = 1$. The analysis can be generalized to many types of modulation including QPSK, M-PAM modulation, and M-QAM as well.

The pdf of $\hat{\gamma}_{\max}$ is [12]

$$f_{\hat{\gamma}_{\max}}(\gamma) = \frac{\partial F_{\hat{\gamma}_{\max}}(\gamma)}{\partial \gamma} = \sum_{n=1}^{N} f_{\hat{\gamma}_n}(\gamma) \prod_{i \neq n}^{N} F_{\hat{\gamma}_i}(\gamma)$$
$$= \sum_{p=1}^{N} \sum_{n=1}^{\binom{N}{p}} (-1)^{p+1} [\Psi^p \mathbf{b}]_n \exp\left(-\gamma [\Psi^p \mathbf{b}]_n\right) \tag{26}$$

where $\mathbf{b} \triangleq \left[\frac{1}{\beta_1}, \frac{1}{\beta_2}, \ldots, \frac{1}{\beta_N}\right]^T$, the matrix Ψ^p is a binary permutation matrix with the dimension of $\binom{N}{p} \times N$, and $(\mathbf{v})_n$ is the n-th element of the vector $\mathbf{v}$. Each row of Ψ^p has p ones and $N-p$ zeros, and it corresponds to one out of $\binom{N}{p}$ possible combination of p ones and $N-p$ zeros.

The average SER for the proposed antenna selection system can be obtained by combining (25) and (26), and the result is

$$\text{SER} = \frac{b}{2} \sum_{p=1}^{N} \sum_{n=1}^{\binom{N}{p}} (-1)^{p+1} \left(1 - \sqrt{\frac{a}{2[\Psi^p \mathbf{b}]_n + a}}\right) \tag{27}$$

where the following identity is used in the derivation of the above equation ([17], Eq. (6.283.2))

$$\int_0^{\infty} Q\left(\sqrt{q\gamma}\right) \exp\left(-p\gamma\right) d\gamma = \frac{1}{2p}\left(1 - \sqrt{\frac{q}{2p+q}}\right) \tag{28}$$

5.3 An average spectral efficiency lower bound

The average spectral efficiency of the system with imperfect CSI is lower bounded by [8]

$$\bar{C} = \int_0^{\infty} \log_2(1+\gamma) f_{\hat{\gamma}_{\max}}(\gamma) d\gamma. \tag{29}$$

Based on the identity, $\int_0^{\infty} \exp(-\alpha x) \log_2(1+x) dx = \frac{1.44}{\alpha} \exp(\alpha) \Gamma(0, \alpha)$ ([17], Eq. (4.337.1)), where $\Gamma(0,x) = \int_x^{\infty} \frac{1}{t} \exp(-t) dt$ is the incomplete Gamma function and the pdf of $\hat{\gamma}_{\max}$ in (26), the average spectral efficiency lower bound can be written as

$$\bar{C} = 0.72 \sum_{p=1}^{N} \sum_{n=1}^{\binom{N}{p}} (-1)^{p+1} \exp\left([\Psi^p \mathbf{b}]_n\right) \Gamma\left(0, [\Psi^p \mathbf{b}]_n\right). \tag{30}$$

5.4 Switching rate

The switching rate is defined as the number of times per second that the system has to switch from one MR antenna to another. It is an important measure on the complexity of the implementation of the antenna selection schemes in practical systems. The switching rates for dual branch [18] and multi-branch [19] systems with perfect CSI have been investigated. In this section, the impacts of channel estimation error on switching rate are analytically studied. Specifically, the switching rate of a two-branch system with independent but non-identically distributed (i.n.d.) branches is mainly investigated.

For a two-branch system, define a new random process

$$Z(t) = R_1(t) - R_2(t) \tag{31}$$

where $R_n(t) = \sqrt{\hat{\gamma}_n(t)}$ is the square root of the estimated SNR at time t. From (16), the pdf of $R_n(t)$ is

$$f_{R_n}(x) = \frac{x}{m_{\hat{\gamma}_n}} \exp\left(-\frac{x^2}{2m_{\hat{\gamma}_n}}\right), \quad \text{for } n = 1, 2 \tag{32}$$

where $m_{\hat{\gamma}_n} = \mathbb{E}[\hat{\gamma}_n]$. From (16), it can be obtained as

$$m_{\hat{\gamma}_n} = \frac{\gamma_n\left(1-\sigma_n^2\right)}{\gamma_n \sigma_n^2 + 1} = \left[\left(1 + \frac{1}{\gamma_n}\right)^2 \frac{1}{J_0^2(2\pi f_n T_0)} - 1\right]^{-1} \tag{33}$$

With the definition of $Z(t)$ in (31), the switching rate can be calculated as [18],

$$\text{SR} = f_Z(0) \left[\int_{-\infty}^{0} |\dot{z}| f_{\dot{Z}}(\dot{z}) d\dot{z} + \int_0^{\infty} \dot{z} f_{\dot{Z}}(\dot{z}) d\dot{z}\right] \tag{34}$$

where $\dot{Z}(t)$ is the derivative process of $Z(t)$, and $f_Z(0) = \int_0^{\infty} f_{R_1}(x) f_{R_2}(x) dx$ is the pdf of $Z(t)$ evaluated at 0.

From (32), $f_Z(0)$ can be calculated as

$$f_Z(0) = \frac{\sqrt{m_{\hat{\gamma}_1} m_{\hat{\gamma}_2}}}{\left(m_{\hat{\gamma}_1} + m_{\hat{\gamma}_2}\right)^{\frac{3}{2}}} \sqrt{\frac{\pi}{2}} \tag{35}$$

The derivative of $Z(t)$, $\dot{Z}(t) = \dot{R}_1(t) - \dot{R}_2(t)$ is zero-mean Gaussian distributed because $\dot{R}_1(t)$ and $\dot{R}_2(t)$ are independent zero-mean Gaussian processes [18], and the variance of $\dot{Z}(t)$ is

$$\sigma_{\dot{Z}}^2 = 2\pi^2 \left(f_1^2 m_{\hat{\gamma}_1} + f_2^2 m_{\hat{\gamma}_2}\right) \tag{36}$$

Therefore, it can be presented as:

$$\int_{-\infty}^{0} |\dot{z}| f_{\dot{Z}}(\dot{z}) d\dot{z} = \int_0^{\infty} \dot{z} f_{\dot{Z}}(\dot{z}) d\dot{z} \tag{37}$$
$$= \int_0^{\infty} \frac{\dot{z}}{\sqrt{2\pi}\sigma_{\dot{Z}}} \exp\left(-\frac{\dot{z}^2}{2\sigma_{\dot{Z}}^2}\right) = \frac{\sigma_{\dot{Z}}}{\sqrt{2\pi}}$$

Combining (34)-(37) yields

$$\text{SR} = \frac{\pi \sqrt{2 m_{\hat{\gamma}_1} m_{\hat{\gamma}_2}} \sqrt{f_1^2 m_{\hat{\gamma}_1} + f_2^2 m_{\hat{\gamma}_2}}}{\left(m_{\hat{\gamma}_1} + m_{\hat{\gamma}_2}\right)^{\frac{3}{2}}} \tag{38}$$

In the above analysis, the outage probability, average SER, average spectral efficiency lower bound, and switching rate are expressed as explicit functions of the average SNR, γ_n, and the channel estimation MSE, σ_n^2, which in turn are functions of the Doppler spread, f_n, and the distance between the antenna and BS. These results analytically quantify the impacts of imperfect CSI and the geometric layout of the distributed antenna array on the

performance of the distributed antenna selection in HSR systems.

6 Numerical and simulation results

Numerical and simulation results are presented in this section to validate the analytical results, and to demonstrate the impacts of imperfect CSI on the performance of HSR systems with the proposed antenna selection scheme. For convenience, $\gamma = \frac{E_0}{d_{\min}^{\alpha}\sigma_z^2}$ is used as the reference received SNR, where $d_{\min}$ is the shortest possible distance between BS antenna and MR antennas. Set $d_{\min} = 60$ m, cell rdius $R = 1000$ m, the length of the rain $L = 400$ m, and path loss exponent $\alpha = 2.3$ in the simulation. BPSK modulation is used for all examples.

Figure 4 shows the outage probability as a function of the reference SNR γ, with various values of the MR antenna number N. The maximum normalized Doppler spread is $f_D T_s = 0.01$ and the horizontal coordinate of the first mobile antenna is $x = 200$. Both analytical and simulation results are shown in the figure, and they match very well in all system configurations. As expected, the outage probability improves with the distributed antenna number N due to the additional spatial diversity. Similar results are also observed for the average symbol error rate and spectral efficiency.

Figures 5, 6, and 7 show the outage probability, average SER, and spectral efficiency lower bound, respectively, under various values of the maximum Doppler spread $f_D T_s$. The number of MR antennas is $N = 4$. All other parameters are the same as the previous example. When $f_D T_s$ is relatively small, the system can obtain an accurate estimate of the fading channel; thus, spatial diversity gains can be obtained by the system. As $f_D T_s$ increases, the performance is dominated by channel estimation errors, and the performance degrades significantly. It can be seen in Figs. 5, 6, and 7 that an error floor appears at high reference SNR when $f_D T_s \geq 0.1$. For example, at $f_D T_s = 0.2$, an error floor at 8×10^{-3} is observed for the outage probability. The error floor is due to channel estimation errors. Therefore, increasing the accuracy of channel estimation or the number of distributed antennas can yield a better performance at the cost of higher complexity.

Figure 8 shows the outage probability as a function of the horizontal coordinate of the first MR antenna, under various values of the maximum normalized Doppler spread $f_D T_s$. The MR antenna number is $N = 4$ and the reference SNR is $\gamma = 10$ dB. It can be seen from Fig. 8 that when the train is close to the base station, both channel estimation error and the antenna-BS distance affect the system performance. When the train is far away from the BS, the impact of path loss dominates the channel gain resulting in a poor performance. It is interesting that the best performance is achieved at the point $x = 200$, which is not the minimum distance between BS and the first antenna. Similar results are also observed for the average symbol error rate and spectral efficiency. Once again, the impact of distance can not be ignored in HSR system.

Figure 9 shows the switching rate as a function of x, the coordinate of the first MR antenna, in a system with $N = 2$ mobile antennas. Systems with different $f_D T_s$ or perfect CSI are considered in this example. For the range of x considered here, the switching rates are quasi-concave in x

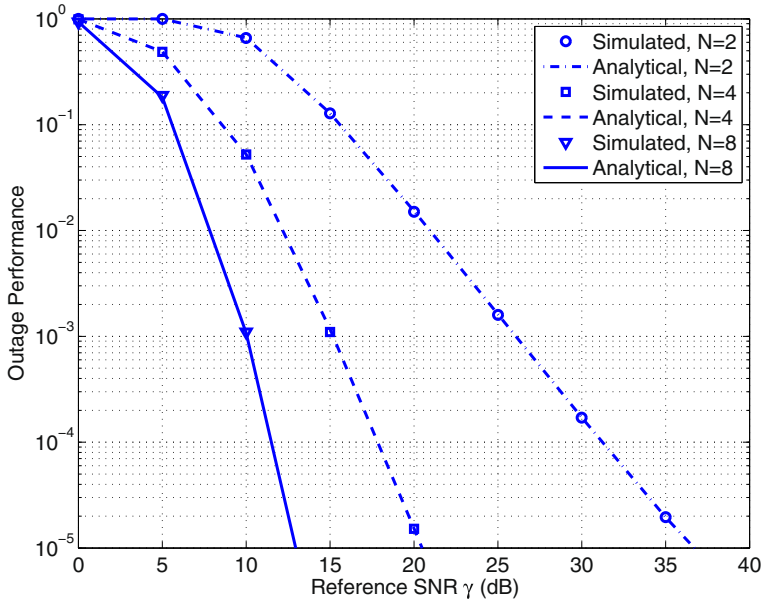

Fig. 4 Outage probability for systems with different number of antennas ($f_D T_s = 0.01$ and $x = 200$)

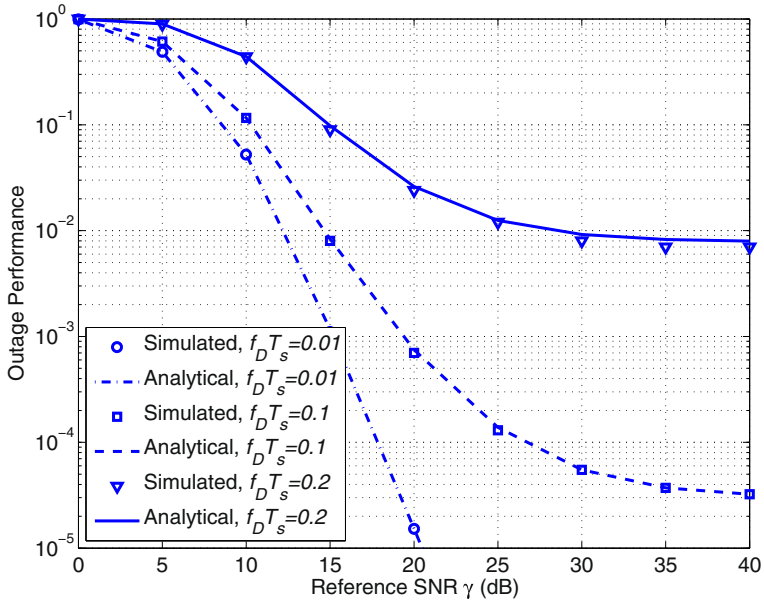

Fig. 5 Outage probability for systems with different maximum normalized Doppler spreads ($N = 4$ and $x = 200$)

for all systems. When x is small, both antennas are close to the BS, and the small-scale fading has a large impact on antenna selection, which leads to large switching rate. When x is large, the fading effect is dominated by pathloss, thus the switching rate decreases at large x. In addition, the impacts of channel estimation error gradually diminish as x becomes large, because of the dominance of the large-scale pathloss.

7 Conclusions

A new antenna selection scheme for HSR systems was proposed in this paper by considering the impacts of imperfect CSI and the geometric layout of distributed antennas mounted on top of the train. The antenna selection was performed by predicting the CSI in the next time slot by following the MMSE criterion. The channel prediction MSE was expressed as a function of the maximum

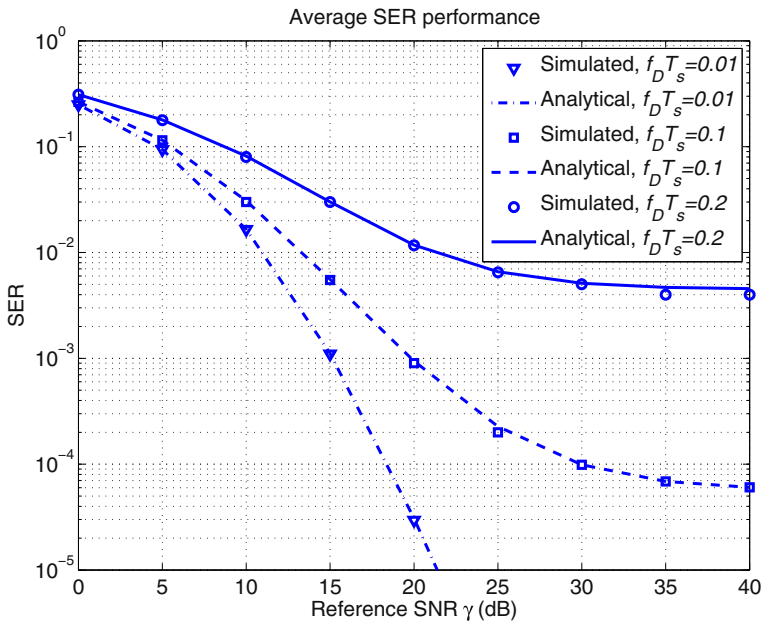

Fig. 6 Average SER for systems different maximum normalized Doppler spread ($N = 4$ and $x = 200$)

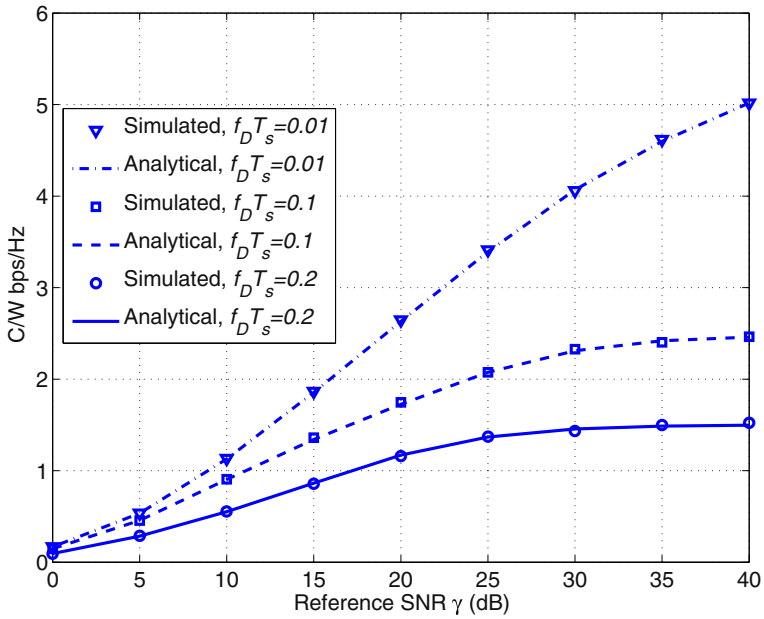

Fig. 7 Spectral efficiency lower bound for systems with different maximum normalized Doppler spread ($N = 4$ and $x = 200$)

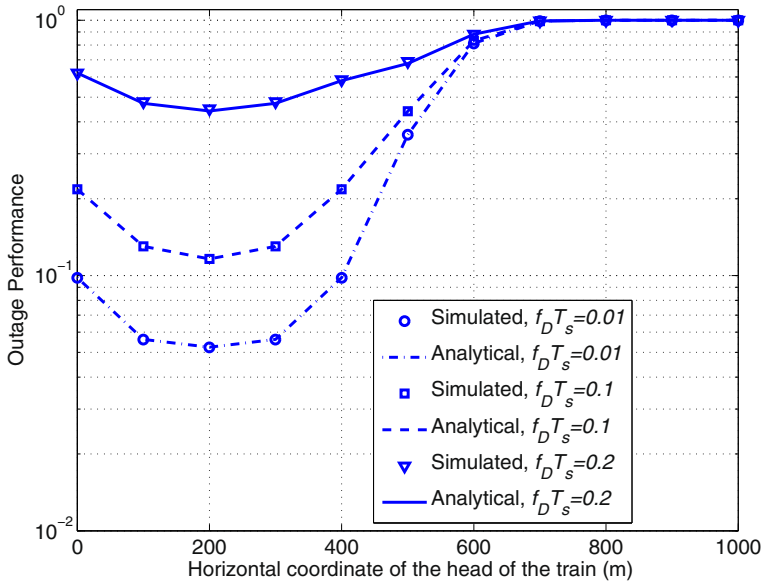

Fig. 8 Outage probability as a function of the horizontal coordinate of the first distributed mobile relay antenna ($N = 4$ and $\gamma = 10$ dB)

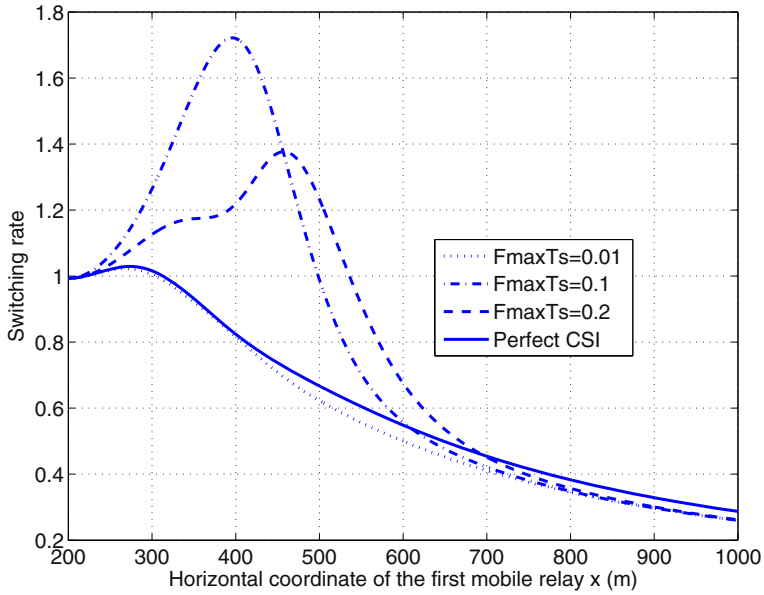

Fig. 9 The switching rate, normalized to the maximum Doppler frequency vs. the horizontal coordinate of the first MR antenna x for different maximum normalized Doppler spread with reference SNR $\gamma = 20dB$

Doppler spread and SNR. The impacts of channel estimation errors and the geometric layout of the antenna on the performance of antenna selections were studied by developing several performance metrics, including the outage probability, the average SER, a spectral efficiency lower bound, and the switching rate. Both analytical and simulation results demonstrated that channel estimation errors have significant impact on the performance of systems with distributed antenna selections.

Abbreviations

AF: Amplify-and-forward; AWGN: Additive white Gaussian noise; BS: Base station; CDF: Cumulative distribution function; CSI: Channel state information; DF: Decode-and-forward; HSR: High-speed railway; MMSE: Minimum mean squared error; ML: Maximum likelihood; MR: Mobile relay; MSE: Mean squared error; OP: Outage probability; pdf: Probability density function; SER: Symbol error rate; SNR: Signal-to-noise ratio; TDD: Time division duplex; UE: User equipment; VPL: Vehicular penetration loss

Funding

The research leading to these results was supported in part by the China-Singapore Joint Research Grant (NSFC-NRF Project) under the grant No. 61661146003/NRF2016NRF-NSFC001-089 and the Innovative Intelligence Base Project (111 Project) under the grant No.111-2-14.

Availability of data and materials

All the results are simulated by the MATLAB.

Authors' contributions

JZ carried out the system model, performed the experiments, and drafted the manuscript. JXW and PZF gave valuable comments on the design of system model and helped in revising the manuscript. All authors read and approved the final manuscript.

Competing interests

The authors declare that they have no competing interests.

Publisher's Note

Author details

[1]Institute of Mobile Communications, Southwest Jiaotong University, 610031 Chengdu, Sichuan, People's Republic of China. [2]Department of Electrical Engineering, University of Arkansas, AR 72701 Fayetteville, USA.

Received: 21 July 2017 Accepted: 12 November 2018
Published online: 04 December 2018

References

1. FuTURE Mobile Communication Forum: White Paper V2.0H 5G Enabler, High mobility support (2016). China
2. P. Fan, J. Zhao, I. Chih-Lin, 5G high mobility wireless communications: challenges and solutions. China Commun. **Supl 2**(13), 1–13 (2016)
3. 3GPP, TR 36.836, V12.0.0, Evolved Universal Terrestrial Radio Access (E-UTRA); Study on Mobile Relay (Release 12) (2014)
4. L. Chen, Y. Huang, F. Xie, Y. Gao, L. Chu, H. He, Y. Li, F. Liang, Y. Yuan, Mobile relay in LTE-advanced systems. IEEE Commun. Mag. **51**(11), 144–151 (2013)
5. A. Khan, A. Jamalipour, Moving relays in hetergeneous cellulaer nerworks-a coverage performance analysis. IEEE Trans. Veh. Technol. **65**(8), 6128–6135 (2016)
6. A. F. Molisch, in *Proceeding Radio and Wireless Conference*. Mimo systems with antenna selection-an overview (IEEE, Boston, 2003), pp. 167–170
7. J. Wu, v P., A survey on high mobility wireless communications: challenges, opportunities and solutions. IEEE Access. **4**, 450–476 (2016)
8. N. Sun, J. Wu, Maximizing spectral efficiency for high mobility systems with imperfect channel state information. IEEE Trans. Wirel. Commun. **13**(3), 1426–1470 (2014)
9. W. Zhou, P. Fan, J. Wu, Energy and spectral efficient doppler diversity transmission in high mobility systems with imperfect channel estimation. EURASIP J. Wirel. Commun. Netw. **1**, 1–12 (2015)
10. W. Zhou, J. Wu, P. Fan, High mobility wireless communications with doppler diversity: fundamental performance limits. IEEE Trans. Wirel. Commun. **14**(12), 6981–6992 (2015)
11. D. S. Michalopoulos, H. A. Suraweera, G. K. Karagiannidis, R. Schober, Amplify-and-forward relay selection with outdated channel estimates. IEEE Trans. Commun. **60**(5), 1278–1290 (2012)

12. M. Seyfi, S. Muhaidat, J. Liang, Amplify-and-forward selection cooperation over rayleigh fading channels with imperfect csi. IEEE Trans. Wirel. Commun. **11**(1), 199–209 (2012)
13. J. L. Vicario, A. Bel, J. A. Lopez-Salcedo, G. Seco, Opportunistic relay selection with outdated CSI: Outage probability and diversity analysis. IEEE Trans. Wirel. Commun. **8**(6), 2872–2876 (2009)
14. Y. Zhou, Z. Pan, J. Hu, J. Shi, X. Mo, in *2011 20th Annual Wireless and Optical Communications Conference (WOCC)*. broadband wireless communications on high speed trains (IEEE, Newark, 2011), pp. 1–6
15. J. Wang, H. Zhu, N. J. Gomes, Distributed antenna systems for mobile communications in high speed trains. IEEE J. Sel. Areas Commun. **30**(4), 675–683 (2012)
16. C. Xiao, J. Wu, S. Y. Leong, Y. R. Zheng, K. B. Lataief, A discrete-time model for triply selective MIMO rayleigh fading channels. IEEE Trans. Wirel. Commun. **3**(5), 1678–1688 (2004)
17. I. S. Gradshteyn, I. M. Ryzhik, *Table of Integrals, Series and Products*. (Academic, American, 2007)
18. N. C. Beaulieu, Switching rates of dual selection diversity and dual switch-and-stay diversity. IEEE Trans. Commun. **56**(9), 1409–1413 (2008)
19. D. S. Michalopoulos, A. S. Lioumpas, G. K. Karagiannidis, R. Schober, Selective cooperative relaying over time-varying channels. IEEE Trans. Commun. **48**(8), 2402–2412 (2010)